Mechanics of Advanced Composite Structures 3 (2016) 45-51

Semnan University

Mechanics of Advanced Composite Structures

journal homepage: http://macs.journals.semnan.ac.ir

On the Study of Mechanical Properties of Aluminum/Nano-Alumina Composites Produced via Powder Injection Molding

H. Abdoos[a*], H. Khorsand[b], A.A. Yousefi[c]

[a] *Department of Nano Technology, Nano-Materials Division, Faculty of New Science and Technology, Semnan University, Semnan, Iran*

[b] *Faculty of Material Science and Engineering, K.N. Toosi University of Technology, Tehran, Iran*

[c] *Iran Polymer and Petrochemical Institute, Tehran, Iran*

PAPER INFO

Paper history:
Received 2016-01-10
Revision Received 2016-03-19
Accepted 2016-04-10

Keywords:
Aluminum matrix composite
Nano-reinforcement
Powder injection molding
Mechanical properties

ABSTRACT

Powder Injection Molding (PIM) is a precision manufacturing process used for production of advanced composites. Mixing of polymeric binder with metal powders, molding of feedstock, de-binding of brown parts and sintering of green samples are four main steps of this process. In the present study, the compounds containing multi-component binder system and aluminum/ nano-alumina (0-9 wt.%) powders were prepared and used as feedstock. After that, the feed-stocks were injected, de-bound and sintered for producing standard specimens. Finally, the sintered composites were produced with a maximum relative density of 97.7%. Afterward, the hardness, yield and ultimate tensile strength of the nano-composites were evaluated. The results showed that the relative density, hardness and strength of the manufactured composites increased due to the addition of nano-reinforcements. It is demonstrated that the effect of alumina on the density of PIM composites differs from that of conventional powder metallurgy. Scanning Electron Microscope (SEM) reveals that the agglomeration takes place in the sample containing 9 wt.% nano-alumina.

1. Introduction

The Aluminum Matrix Composites (AMCs) are desirable metal matrix composites for the automotive, aerospace, defense and electronic industries because of their low density, high specific stiffness, corrosion resistance, high toughness, fatigue resistance, controllable expansion coefficient, and high thermal as well as electrical conductivity [1-3].

The Powder Injection Molding (PIM) is an advanced powder technique that is commonly used for the fabrication of small and delicate composite parts. PIM can significantly decrease the production costs of composites for commercial applications [4]. Feedstock preparing, molding, de-binding and sintering are the four main steps of the PIM. In practical applications the demands for miniaturization, especially in mobile devices such as laptops and cell phones, result in production of heat sinks with different geometries and shape complexity through Al PIM [5,6].

In the case of structural applications, where higher strength and ductility are important, the use of nano-composites is reasonable [7]. Enhancement of the sinterability, improvement of the mechanical properties and fine microstructures are the most significant consequences of nanoparticles in powder technology [8,9]. The feedstock flow and mold filling requirements dictate that only particles or short fibers reinforced composites can be processed by the PIM [4].

Several studies have investigated the presence of additive particles in the flow behavior of powder-polymer mixtures and the properties of PIM products [8,10-15]. The presence of fine particles in the powder-polymer mixtures affects the rheological behavior, because nano-additives usually show poor

* Corresponding author, Tel.: +98-912-6310730; Fax: +98-23-31533302

E-mail address: hassan.abdoos@gmail.com

packing behavior and significantly influence the homogeneity and viscosity of feed-stocks [8]. Torque rheometry, rheological analysis of Al powder-polymer mixtures and the effect of alumina nanoparticles on the rheological behavior of feed-stocks were completely investigated in our previous studies [16,17].

The aluminum-based PIM composites were produced and evaluated by Liu et al. [18,19], Ahmad [20,21] and Adomphol et al. [22]. The sintering temperature, tin addition and heat treatment effect on the density and mechanical properties of 6061 alloy was investigated [18]. Liu et al. [19] also evaluated the mechanical properties and microstructure of injection molded AMCs reinforced with 10 %wt. AlN particles. Ahmad [20], reported the optimum injection parameters for achieving the highest level of fiber orientation in a given direction. He [21], also investigates and determines the injection machine parameters which lead to the formation of defects consisting of voids, cracks and blisters for Al-based material. Adomphole et al. [22], characterized the feedstock for powder injection molding of SiCp-reinforced aluminum composite. They found that the high solid loading was improved by the bulk density while the hardness values were observed to be similar. However, the effect of reinforcement on the mechanical properties of Al-Al_2O_3 PIM nanocomposites has not been addressed yet.

The present study focused on the use of the PIM process for manufacturing the AMCs that were reinforced with nano-aluminum oxide. The Al_2O_3 particles are favored as reinforcements because of their low price, superior high temperature mechanical properties and excellent oxidation resistance that avoid formation of the undesirable phases [23,24]. Furthermore, the effect of nanoparticles on the density and mechanical properties of molded Al-based composites was investigated.

2. Materials and Methods

Al (d_{50} = 25 μm), Sn (d_{50} = 15 μm) and Mg (d_{50} = 11 μm) powders in commercial purity (supplier: Pourian Chem. Co.) were used as starting materials for preparation of pre-mixed Al-2Sn-1Mg (wt.%) powder. The addition of elements such as Mg and Sn as oxygen reactor and sintering activator can be aided by the densification of Al powder [18,19,25].

The chemical composition of the Al powder and particle size distribution parameters, obtained using a Malvern (ZEN3600) particle size analyser, are listed in Table 1.

Table 1. The chemical composition and particle size distribution of powder.

Chemical Composition				Particle size parameters			
Al	Si	Fe	Other	d_{10} (μm)	d_{50} (μm)	d_{90} (μm)	S_w
99.5	0.15	0.15	0.2	12	25	52	4.02

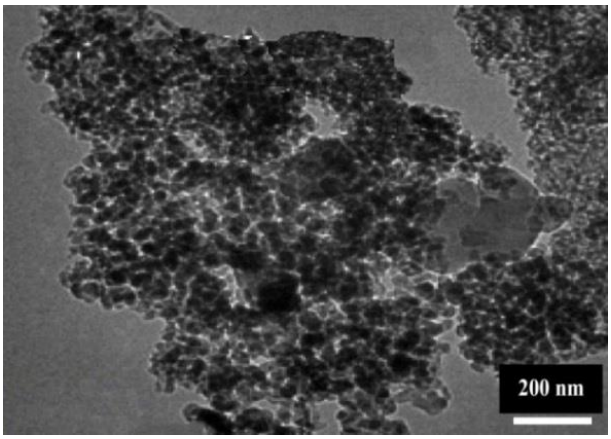

Figure 1. The Transmission Electron Microscope (TEM) image of nanoalumina.

Then; 3, 6 and 9 (wt.-%) α-phase Al_2O_3 (80 nm; >99% purity, supplier: US Research Nanomaterials, USA) was mixed with Al-based powder using a planetary high energy ball mill for 40 min in the presence of ethanol. The TEM image of alumina nano-sized powder is displayed in Fig. 1.

The binder system was comprised of three principal components: poly- propylene (35 vol.%) as a backbone polymer, paraffin wax (60 vol.%) as a plasticizer, and stearic acid (5 vol.%) as a surfactant. The multi-component binder results in gradual and selective binder removal during de-binding. A Brabender mixer (W50) with a pair of rotating blades was used to prepare the feed-stocks. The temperature, speed, and time were optimized during mixing to 180°C, 50 rpm, and 15-45 min, respectively. The mixing process continued until the torque stabilized at a steady state level. Then, the feedstock crushed into granules. The compositions of the prepared feed-stocks are summarized in Table 2. Fig. 2 exhibits, schematically, the materials and feedstock preparation steps.

The standard flat specimens [26] were injected using a Dynisco laboratory mixing molder. The binders were removed in two steps consisting of solvent and thermal de-binding. First, the injected parts were immersed in n-heptane solvent at 55 °C for 6 hours; then the direct thermal de-binding was done according to a heating cycle as shown in the left side of Fig. 3.

The parts were then heated from 500 to 620 °C at a rate of 5 °C/min and also were sintered at 620°C for 1 hour in a nitrogen atmosphere (Fig. 3, right side). The heating regime was adjusted based on the binder decomposition temperatures. Thermal properties of the binder's constituents were determined by Thermal Gravimetric Analysis (TGA) equipment (PL-TGA) according to the ASTM E 1113 standard [27].

A scanning electron microscope (FE-TESCAN, Mira II, 15.00 kv) was utilized for microstructural investigation of the samples. The density was measured based on the Archimedes immersion technique.

Table 2. The different feedstock compositions for experiments.

Symbol	Powder Loading (vol.-%)	Powder Composition (wt.-%)		Binder Volume (vol.-%)
		Al	Alumina	
Al60	60	100	0	40
Al-3NP-60		97	3	
Al-6NP-60		94	6	
Al-9NP-60		91	9	

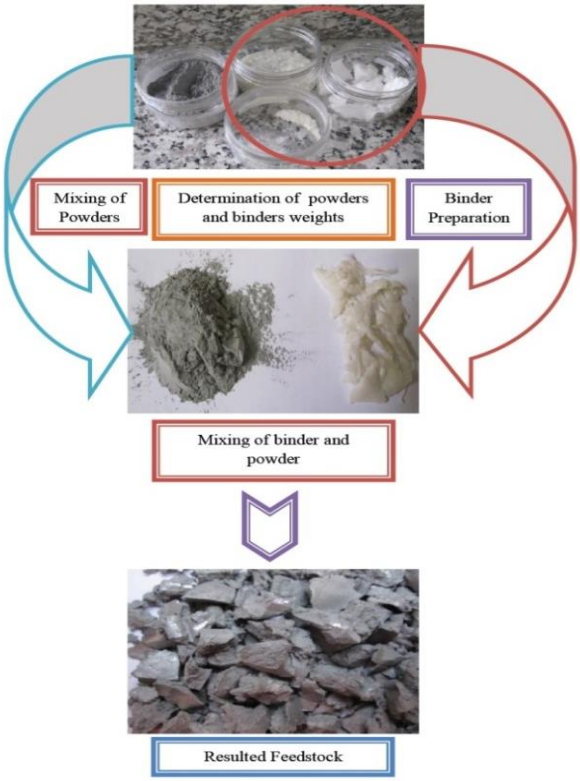

Figure 2. The schematic of feed-stock preparation process.

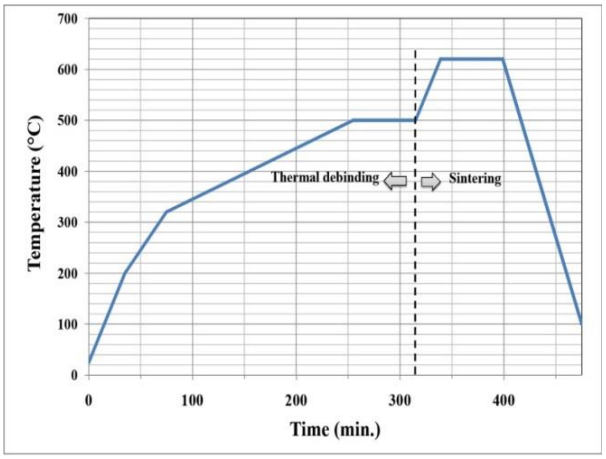

Figure 3. The thermal de-binding and sintering heating cycles.

The hardness and tensile tests were performed according to MPIF 43 [28] and ASTM D 1708 [26], respectively.

3. Results and Discussion

Fig. 4 is a micrograph of the feedstock which shows the powder particles covered by a thin layer of polymeric binder.

Fig. 5 shows the optical images of the produced specimens. After sintering, the parts are free of defects such as cracks and blisters. The isometric and proportional shrinkage can be seen in the sintered parts. The powder densification takes place for all samples during the sintering cycle.

For example, Fig. 6 shows the SEM image of sintered specimen which in turn indicates the consolidated surface.

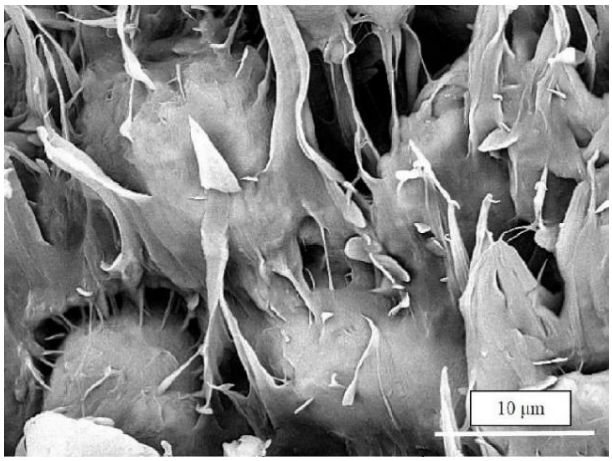

Figure 4. The SEM micrograph of the prepared powder-polymer mixtures.

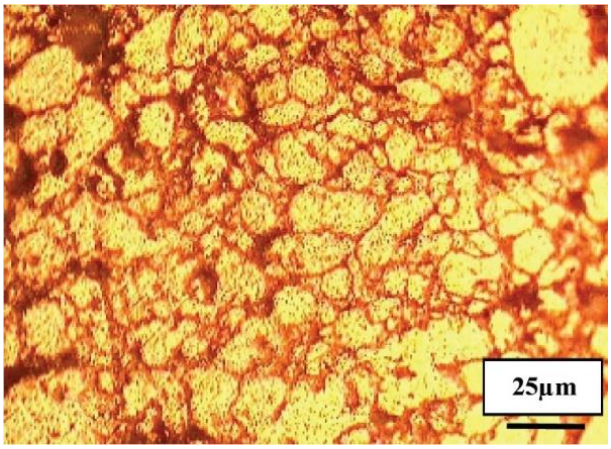

Figure 5. The optical images of the injected, green and sintered parts.

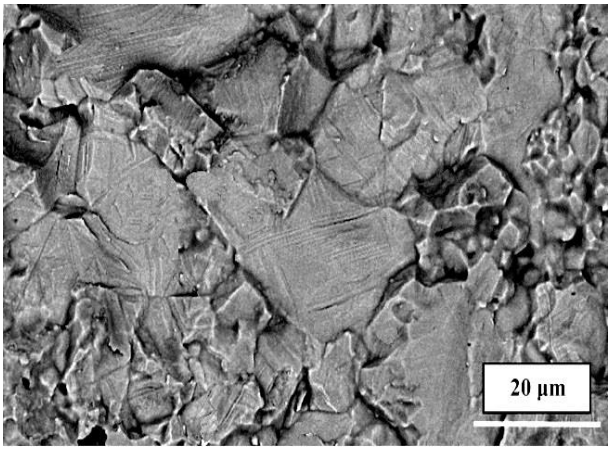

Figure 6. The SEM image of the sintered surface.

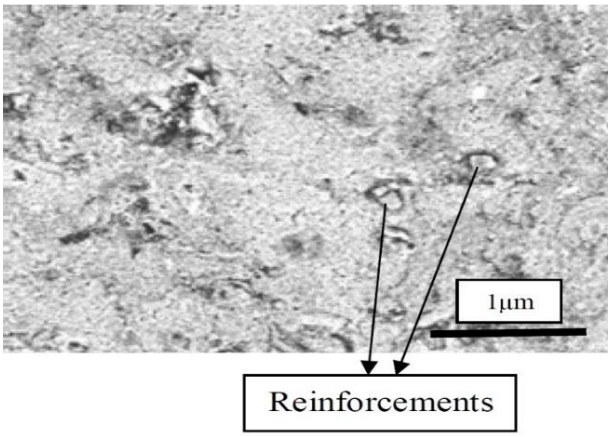

Figure 7. The general microstructure of the injected Al-based nano-composites (matrix: Al, reinforcements: nano-alumina).

The general microstructure, FE-SEM image of the produced nano-composites is presented in Fig. 7. The aluminum oxide nanoparticles can be discerned in this figure. Furthermore, an optical image is shown in Fig. 8, which in turn shows the general microstructure feature consists of the powder particles and the pores. The relative densities of the various composites after sintering are shown in Fig. 9 and are varied from 95.8% to 97.7%.

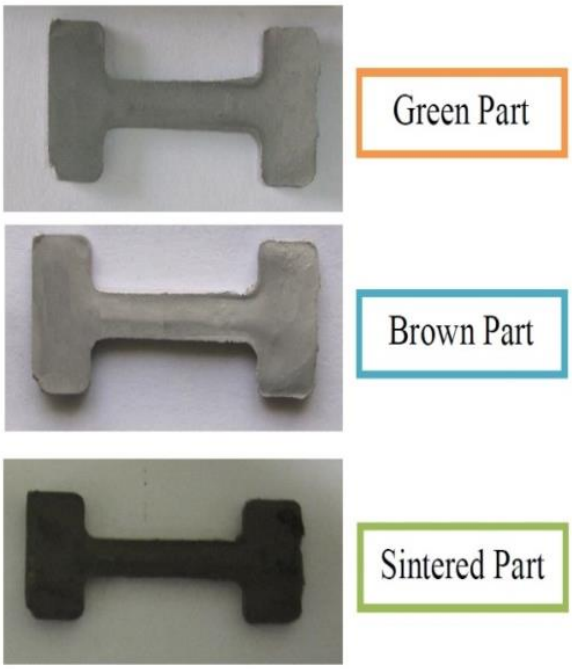

Figure 8. The optical image of the produced sample consisting powder particles and pores.

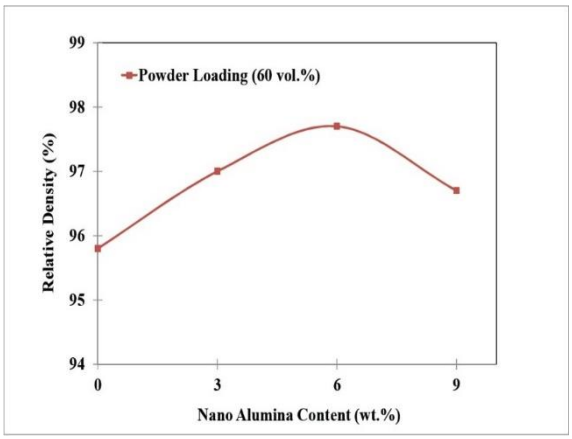

Figure 9. The relative density against the contents of nano-alumina.

The density of alumina is 3.95 g/cm^3 and consequently higher than Al powder. However, in conventional powder metallurgy, when the alumina content increases, the relative density of the Al-based composites decreases, as reported by Rahimian et al. [23]. The compressibility of the composite powder declines due to increasing the reinforcement, since the hardness of alumina is higher than Al, which results in increment of friction between particles. Inversely, in the PIM, the mold cavity is filled with a uniform and hydrodynamic pressure and the densification of the composite powder is not restricted by higher hardness of alumina. The nano-additives can fill the interstices among larger particles and increase the packing and relative density.
However, in the PIM, the agglomeration of fine powders can obstruct more densification [8,12], as a

result of which, the relative density decreases with the addition of 9% nano-alumina. Figure 10 shows the distribution of reinforcement particles in two de-bound samples. The powder agglomeration can obviously be seen in the specimen containing 9 wt.-% nano-alumina. When the fine powder ratio increases, more binder is required to provide essential flowability, because of the increased surface area. Therefore, it appears that in Al-9NP-60, there is an inadequate amount of binder for flowability and movement of the nanoparticles through the interstices of the Al powders. Consequently, the agglomeration of alumina and hence decreasing of relative density occur as the particle packing decreases. Decreasing the density in Al-9NP-60 can also affect other mechanical properties such as yield and ultimate tensile strength (refer to Figs. 11 and 12).

The hardness, yield and ultimate tensile strength (UTS) are shown in Figs. 11 and 12. Adding nano-alumina as reinforcement considerably enhances the mechanical properties of aluminum matrix as seen in the aforementioned figures (except Al-9NP-60). Generally, the nano-additives persuade sintering process, create finer microstructures and make better tolerance control [8,29]. It is described that the strength of an aluminum matrix increases with decreasing the reinforcement's size from micrometer to nanometer, at least 20% [9]. In other words, the effect of reinforcement size on the mechanical behavior is recognized and proved [23,30]. It reveals that decreasing the particle size increases the mechanical properties of the composites.

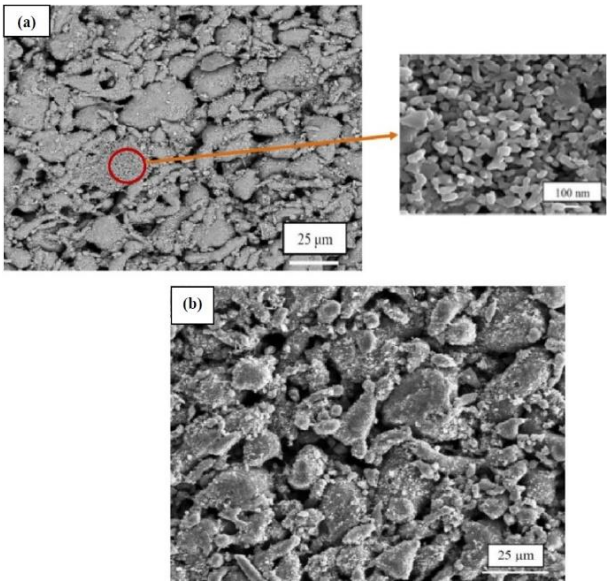

Figure 10. The distribution of secondary phase in two de-bound samples containing different nanoalumina amounts as reinforcement (a) 9 wt. % in high and low magnification indicating agglomeration and (b) 6 wt.%.

This issue can be explained from two perspectives. First, with decreasing the reinforcement size to nanometer, the interface between the soft matrix and the hard nano-phase gets higher. Second, the strength of nanoparticles against fracture, under the loading, is higher than coarser particle due to few defects. Therefore, the nanoparticles have higher hardness and strength in comparison with the coarser particles [31].

As it can be seen, the hardness, yield, strength and UTS increase with addition of nano-alumina. In metal matrix composites, the dislocation movement is prevented by dispersion strengthening mechanism. Thus, the level of matrix strengthening depends on the distance, mode of distribution and the amount and size of the secondary phase [32].

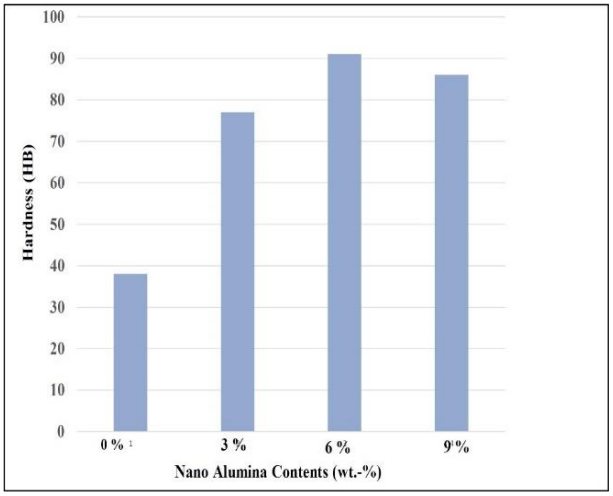

Figure 11. The hardness of Al-based composites against the nanoparticle contents.

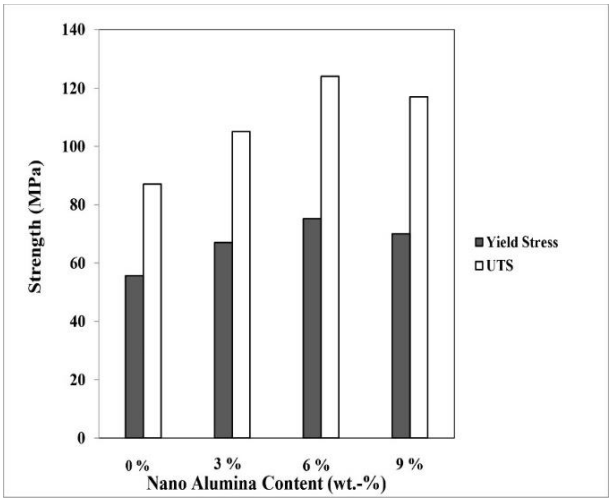

Figure 12. The strength of Al-based composites against the nanoparticle contents.

For particulate composites having uniform distribution of the secondary phase, the relation among interspacing of the reinforcement (λ), volume fraction (f) and diameter (r) is as below [33]:

$$\lambda = \frac{4\,(1-f)r}{3f} \quad (1)$$

Therefore, the space between the second particles decreases with increasing the reinforcement weight fraction. On the other hand, the required stress for dislocation movement, between two adjacent alumina particles which determines the material strength, increases due to the less interspacing of particles [23]:

$$\tau_0 = \frac{Gb}{\lambda} \quad (2)$$

Where, τ_0 , G and b are the required tension stress for forcing dislocation to move through reinforcement particle, material's modulus and Berger's vector, respectively.

On the other hand, the Hall-Petch type expression for the hardness of the composite (H_c) is as below [34]:

$$H_c = \rho_{fc}\left(H_m + \frac{\emptyset_p^{0.5}(H_p - H_m)}{d^{0.25}}\right) \quad (3)$$

Where ρ_{fC}, H_m, Φ_p, H_P and d are the composite relative density, matrix hardness, volume fraction of particulate reinforcement, hardness of reinforcement and particle diameter, respectively.

The fracture strength of the composite (σ_C) is assumed to follow a relation analogous to the hardness [35]:

$$\sigma_C = \rho_{fc}\left(\sigma_m + \frac{\emptyset_p^{0.5}(\sigma_p - \sigma_m)}{d^{0.25}}\right) \quad (4)$$

Where, σ_p and σ_m are the fracture strengths of the matrix and particulate reinforcement, respectively.

According to equations (3) and (4), it is expected that the hardness and strength of a metal matrix composite increase with increasing the reinforcement volume fraction, as seen in above equations for Al- nano-alumina composite.

4. Conclusions

The mechanical behaviors of Al-based nanocomposites were studied in the present study. After the injection, the combination of the solvent and thermal de-binding was performed for the binder removal. The sound parts having relative sintered densities in the range of 95.8% to 97.7%, were produced. The mechanical properties of composites were improved due to the addition of nanoreinfoecement. The agglomeration of nanoparticles, due to inadequate amounts of binder, was seen in Al-9NP-60 which caused a reduction in the Al-9NP-60 mechanical properties.

Acknowledgements

The authors wish to thank Iran polymer and petrochemical institute for cooperation and providing the experimental facilities.

References

[1] Rahimian M, Parvin N, Ehsani N. Investigation of particle size and amount of alumina on microstructure and mechanical properties of Al matrix composite made by powder metallurgy. *Mater Sci Eng A* 2010; 527(4):1031-1038.

[2] Tatar C, Ozdemir N. Investigation of thermal conductivity and microstructure of the α-Al_2O_3 particulate reinforced aluminum composites (Al/Al_2O_3-MMC) by powder metallurgy method. *Phys B Condensed Matter* 2010, 405(3): 896-899.

[3] Su H, Gao W, Feng Z, Lu Z. Processing, microstructure and tensile properties of nano-sized Al_2O_3 particle reinforced aluminum matrix composites. *Mater Des* 2012, 36: 590-596.

[4] Ye H, Liu XY, Hong H. Fabrication of metal matrix composites by metal injection molding - A review. *J Mater Process Technol* 2008, 200(1): 12-24.

[5] Johnson JL, Tan LK. **Metal injection molding of heat sinks**. Electronics cooling, 2004.

[6] The A to Z of Materials Science (AZO Materials), AluMIM, Aluminum Injection Molding from Advanced Materials Technologies (AMT), Archive of Articles, 2004, http://www.azom.com /article.aspx? ArticleID = 2396.

[7] Hesabi ZR, Simchi A, Reihani SS. Structural evolution during mechanical milling of nanometric and micrometric Al_2O_3 reinforced Al matrix composites. *Mater Sci Eng A* 2006, 428(1): 159-168.

[8] Onbattuvelli VP, Enneti RK, Park SJ, Atre SV. The effects of nanoparticle addition on SiC and AlN powder–polymer mixtures: Packing and flow behavior. *Int J Refractory Metals and Hard Mater* 2013, 36: 183-190.

[9] Jia DC. Influence of SiC particulate size on the microstructural evolution and mechanical properties of Al-6Ti-6Nb matrix composites. *Mater Sci Eng A* 2000, 289(1): 83-90.

[10] Onbattuvelli VP, Enneti RK, Atre SV. The effects of nanoparticle addition on the sintering and properties of bimodal AlN. *Ceram Int* 2012, 38(8): 6495-6499.

[11] Onbattuvelli VP, Enneti RK, Atre SV. The effects of nanoparticle addition on the densification and properties of SiC. *Ceram Int* 2012, 38(7): 5393-5399.

[12] Khakbiz M, Simchi A, Bagheri R. Analysis of the rheological behavior and stability of 316L stainless steel–TiC powder injection molding feedstock. *Mater Sci Eng A* 2005, 407(1): 105-113.
[13] Huang B, Fan J, Liang S, Qu X. The rheological and sintering behavior of W–Ni–Fe nano-structured crystalline powder. *J Mater Process Technol* 2003, 137(1): 177-182.
[14] Kim Y, Lee S, Noh JW, Lee SH, Jeong ID, Park SJ. Rheological and sintering behaviors of nanostructured molybdenum powder. *Int J Refractory Metals and Hard Mater* 2013, 41: 442-448.
[15] Olhero SM, Ferreira JM. Influence of particle size distribution on rheology and particle packing of silica-based suspensions. *Powder Technol* 2004, 139(1): 69-75.
[16] Abdoos H, Khorsand H, Yousefi AA. Torque rheometry and rheological analysis of powder–polymer mixture for aluminum powder injection molding. *Iranian Polym J* 2014, 23(10): 745-55.
[17] Abdoos H, Khorsand H, Yousefi AA. Effect of alumina nanoparticles on the rheological behavior of aluminum-binder mixtures for powder injection molding. *Iranian J Polym Sci Technol*2014, 27(4): 313-324.
[18] Liu ZY, Sercombe TB, Schaffer GB. Metal injection molding of aluminum alloy 6061 with tin. *Powder Metall* 2008, 51: 78-83.
[19] Liu ZY, Kent D, Schaffer GB. Powder injection moulding of an Al–AlN metal matrix composite. *Mater Sci Eng A.* 2009, 513: 352-356.
[20] Ahmad F. Orientation of short fibers in powder injection molded aluminum matrix composites. *J Mater Process Technol* 2005, 169: 263-269.
[21] Ahmad F. Control of defects in powder injection molded aluminum matrix composites. *Int J Powder Metall* 2008, 44(3): 69-76.
[22] Udomphol T, Inpanya B, Chuankrerkkul N. Characterization of Feedstocks for Injection Molded SiC_p-Reinforced Al-4.5 wt.% Cu Composite. *Adv Mater Res* 2011, 383: 3234-3240.
[23] Rahimian M, Parvin N, Ehsani N. Investigation of particle size and amount of alumina on microstructure and mechanical properties of Al matrix composite made by powder metallurgy. *Mater Sci Eng A.* 2010, 527(4): 1031-1038.
[24] Hassan SF, Gupta M. Development of high performance magnesium nano-composites using nano-Al_2O_3 as reinforcement. *Mater Sci Eng A* 2005, 392(1): 163-168.
[25] Zlatkov BS, Griesmayer E, Loibl H, et al. Recent advances in PIM technology I. *Sci Sintering* 2008, 40(1): 79-88.
[26] ASTM D1708–02a, **Standard test method for tensile properties of plastics by use of microtensile specimens**, ASTM International, 2002
[27] ASTM E1131, **Standard test method for compositional analysis by thermo-gravi-metry**, ASTM International, 2005.
[28] MPIF 43, **Method for determination of apparent hardness of powder metallurgy products**, Metal Powder Industries Federation (MPIF), 2010.
[29] Kim KH, Lee BT, Choi CJ. Fabrication and evaluation of powder injection molded Fe–Ni sintered bodies using nano Fe-50% Ni powder. *J Alloys Compd* 2010, 491(1): 391-394.
[30] Sevik H., Kurnaz SC. Properties of alumina particulate reinforced aluminum alloy produced by pressure die casting. *Mater Des* 2006, 27(8): 676-683.
[31] Gleiter H. Nanostructured materials: basic concepts and microstructure. *Acta Mater* 2000, 48(1): 1-29.
[32] Rajkovic V, Bozic D, Jovanovic MT. Properties of copper matrix reinforced with nano-and micro-sized Al_2O_3 particles. *J Alloys Compd* 2008, 459(1): 177-184.
[33] Dieter GE, Bacon D. **Mechanical metallurgy**. McGraw-Hill, 1986.
[34] Miller WS, Humphreys FJ. Strengthening mechanisms in particulate metal matrix composites. *Scripta Metall Mater* 1991, 25(1): 33-38.
[35] Johnson JL. Opportunities for PM Processing of Metal Matrix Composites. *Int J Powder Metall* 2011, 47(2): 19-28.